

修士論文

Dynamical models of bubble-bubble interactions

in isothermal and boiling systems

等温系及び沸騰系における気泡間干渉の動的モデル

1 - 50 ページ 完

平成 16年 2月 13日 提出

指導教官 庄司 正弘 教授

26177 氏名 丹下 学

Master's Thesis

Dynamical Models
of
Bubble-bubble Interactions
in
Isothermal and Boiling Systems

by

Manabu Tange

*Department of Mechanical Engineering,
Graduate School of Engineering*

2004, The University of Tokyo, Japan

Abstract

This master's thesis examines the essences of the interactions between generated bubbles in isothermal system and boiling system.

In isothermal system, gas bubbles were generated from twin orifices submerged in water. Bubbling features were observed using high-speed video. At each orifice, a hot wire anemometer detected the micro-convection induced by successively generated bubbles. It is found that bubbling pattern differs depending on the chamber volume as well as the air volumetric flow rate. When the chamber volume is small and the flow rate is relatively low, "reciprocal" and "counterpart" bubbling patterns repeatedly appear with gradual decreasing the air flow rate. Between the two patterns, "aperiodic" bubbling takes place. To reveal the mechanism of such interactive bubbling features, a simplified theoretical model is proposed. It describes the time evolution of individual bubble volume basing on the equations of motion for gas and liquid. The distribution of air flow into two bubbles is uneven and yields various bubbling patterns. The model explains well the appearance of three bubbling patterns and their repetition.

In boiling system, vapor bubbles were generated from two nucleation sites on an artificial surface. Experiment revealed that average bubbling frequency and bubbling periods distribution changed if a cavity spacing, an intensity of the interaction, was varied. In order to reproduce and understand the interaction, a simple dynamical model similar to that in isothermal system, was constructed. It describes the temperature, bubble volume and previous bubble motion on each site. Nevertheless it made the bubbling periods distribution, clear dependence of cavity spacing is not shown. Further improvements of the model are required.

Acknowledgment

I sincerely express gratitude to prof. Masahiro Shoji, my supervisor, for his generous help in preparing this thesis. When I worried myself too much over my future specialty I would major in, I read a essay [1] written by him in a journal. In the essay, he said that engineering researchers should study more individually and more easily. I was moved to action by what he said, and chose to study under him in my master's course.

I would also like to acknowledge prof. Shigeo Maruyama for his helpful and piercing comments at research meetings. His penetrating comments pointed out where the problem of my model was and helped me strike out in new directions.

I would like to acknowledge with much thanks Dr. Zhang and Mr. Shimura for their fantastic experimental results which gave me impulses of modeling. I would like to appreciate Mr. Watanabe and Mr. Miyazaki for their kind help in performing the experiment and Dr. Matsumoto at AIST (national institute of advanced industrial science and technology) for fabrication of cavities on silicon surfaces. I could not have conducted all experiments without their helps.

Hearty gratitude should be expressed to the members of our laboratory, especially Dr. Ito, Dr. Shibuta and Mr. Miyauchi, who have discussed all things of research and study.

Finally I am most indebted to my parents who have supported my living and my dreams.

Contents

Nomenclature	8
1 Introduction	10
1.1 Introduction of Nucleate Boiling	10
1.2 Introduction of Interaction	11
1.3 Dynamical Behavior of Boiling	13
1.4 Past Researches of Artificial Surface in Our Laboratory	14
1.5 Objectives	15
2 Interaction in Isothermal System	16
2.1 Introduction	16
2.2 Experimental Apparatus	17
2.3 Experimental Results	18
2.3.1 Bubbling pattern at low flow rate	18
2.3.2 Pattern transition	21
2.3.3 Power law for pattern transition	22
2.4 Simplified Theoretical Model	22
2.4.1 Assumptions	22
2.4.2 Phenomenological governing equations	24
2.5 Model Behavior	25
2.5.1 Configuration space and phase space	25
2.5.2 Effect of surface tension	26
2.5.3 Effect of inertial force	27
2.5.4 Growth of twin bubbles and trajectory on configura- tion space	28
2.5.5 Simulated spectrogram and power law	29
2.6 Concluding Remarks	29
3 Interaction in Boiling System	32
3.1 Introduction	32
3.2 Experimental Setups	33
3.3 Experimental Results	33

3.3.1	Bubbling frequency[26]	33
3.3.2	Distribution of bubbling periods	34
3.3.3	Photographic observation	35
3.4	Simplified Theoretical Model	37
3.4.1	Problem statement	37
3.4.2	Assumptions	38
3.4.3	Phenomenological governing equation	42
3.5	Model Behavior	42
3.6	Concluding Remarks	44
4	Conclusion	45
	Bibliography	46

List of Figures

1.1	Boiling curve [2].	11
1.2	Analogy of bubbling between isothermal system and boiling system.	12
1.3	Actual boiling surface and interaction.	12
1.4	Analogy of bubble-bubble interactions between isothermal system and boiling system.	13
1.5	Coupled map lattice of boiling [10]	14
2.1	Sketch of experimental setups	18
2.2	Snapshots of major bubbling patterns.	19
2.3	Time series of bubble volume and power spectrum of each bubbling pattern.	20
2.4	Spectrogram of wire probe signal.	21
2.5	Flowrate at pattern transition(experiment).	22
2.6	Sketch and notation of idealized bubble shape	23
2.7	A typical example of trajectory on configuration space.	26
2.8	A typical example of trajectory on phase space.	27
2.9	Pressure difference with surface tension.	28
2.10	Time series of bubble volumes and phase space expression.	29
2.11	Spectrogram of simulation results.	30
2.12	Flow rate at pattern transition of simulation results.	30
3.1	Schematic diagram of experimental system of nucleate pool boiling on artificial surface	34
3.2	Bubbling frequency and three dominant factors	35
3.3	Bubbling period distribution (Experiment)	36
3.4	Vertical coalescence	36
3.5	Horizontal coalescence.	37
3.6	Declining coalescence	37
3.7	Notation of bubble condition	39
3.8	Bubbling period distribution (Model)	43

Nomenclature

Roman letters

- A : area, m^2
 $\text{Bi} := hL/k$, Biot number, –
 C_D : drag coefficient, –
 c : specific heat, J/kg K
 c_p : specific heat at constant pressure, J/Kg K
 D : diameter, m
 f : force, N
 $\text{Fo} := \alpha t/L^2$, Fourier number, –
 g : gravitational acceleration, m/s^2
 h : heat transfer coefficient, $\text{W/m}^2\text{K}$
 h_{fg} : enthalpy of vaporization, J/kg
 $\text{Ja} := \rho_\ell c_{p,\ell} \Delta T / \rho_v h_{\text{fg}}$, Jacob number, –
 k : thermal conductivity, W/mK
 $L_c := \sqrt{\sigma / (\rho_\ell - \rho_v) g}$, capillary length, m
 $\text{Nu} := hL/k$, Nusselt number, –
 P : pressure, Pa
 $\text{Pr} := \nu / \alpha$, Prandtl number, –
 q : volumetric gas flow rate in chap. 2, m^3/s ,
heat flux in chap. 3, W/m^2
 r : bubble radius of curvature, m
 S : spacing between orifices in chap. 2, m
spacing between cavities in chap. 3, m
 T : temperature, K
 t : time, s
 u : velocity, m/s
 V : bubble volume, m^3

Greek letters

- α : thermal diffusivity, m^2/s
- δ : thickness of orifice, m
- δ_{th} : thickness of superheated liquid layer, m
- γ : width of temperature distribution
- $\theta := \sin^{-1}(D/2r)$, rad
- μ : viscosity, $\text{Pa} \cdot \text{s}$
- ν : dynamical viscosity, m^2/s
- ρ : density, kg/m^3
- σ : surface tension, N/m

Subscripts on any variable, Q :

- Q_{c} : value for chamber
- Q_{d} : value for detachment
- Q_i : value for orifice i in chap. 2 and site i in chap. 3 ($i = 1, 2$)
- Q_{g} : value for gas
- Q_{ℓ} : value for liquid
- Q_{v} : value for vapor
- Q_{pre} : value for previous bubble
- Q_{wake} : value for wake

Superscripts on any variable, Q :

- \bar{Q} : mean value of Q
- \dot{Q} : time derivative of Q
- \ddot{Q} : second time derivative of Q
- Q^* : dimensionless value of Q

Chapter 1

Introduction

1.1 Introduction of Nucleate Boiling

Nucleate boiling has been extensively utilized in industry in view of the fact that it is one of the most efficient heat transfer modes, particularly in high energy density systems, such as nuclear power plants, boiler and the like. These conventional applications intensely need the useful correlation functions like $\bar{q} = f(\bar{T})$, namely “boiling curve” as shown in Fig. 1.1[2]. Here, \bar{q} and \bar{T} are average heat flux and average surface temperature, respectively. In other words, all correlations took the average properties in time and in space. Heat transfer of nucleate boiling is correlated mainly from experiments due to highly nonlinear behavior of vapor bubble while some other convectional flows correlated from analytical methods [3].

In recent years, however, the spatio-temporal (in space and in time) understanding of boiling behavior has come to be required (Shoji [4] proposed a vision of “boiling chaos”). Cooling of a recent electric device with boiling heat transfer will be required for its large heat generation since air cooling is not enough to maintain the temperature of the devices. Traditional boiling researches paying attention to average heat transfer properties cannot give sufficient solutions since the size of the cooled surface is comparable with bubble radius and heat transfer become highly transitional.

One of the techniques to facilitate the interaction of boiling is to separate the complexities into hydrodynamical part and thermal part. In other words, It is effectual to investigate bubble dynamics and its interaction of gas-liquid system without phase change, isothermal system. Takagi and Shoji [5] presented an analogy of bubble behavior between isothermal and boiling system. Heat flux and surface temperature in boiling system correspond to gas flow rate and chamber pressure in isothermal system.

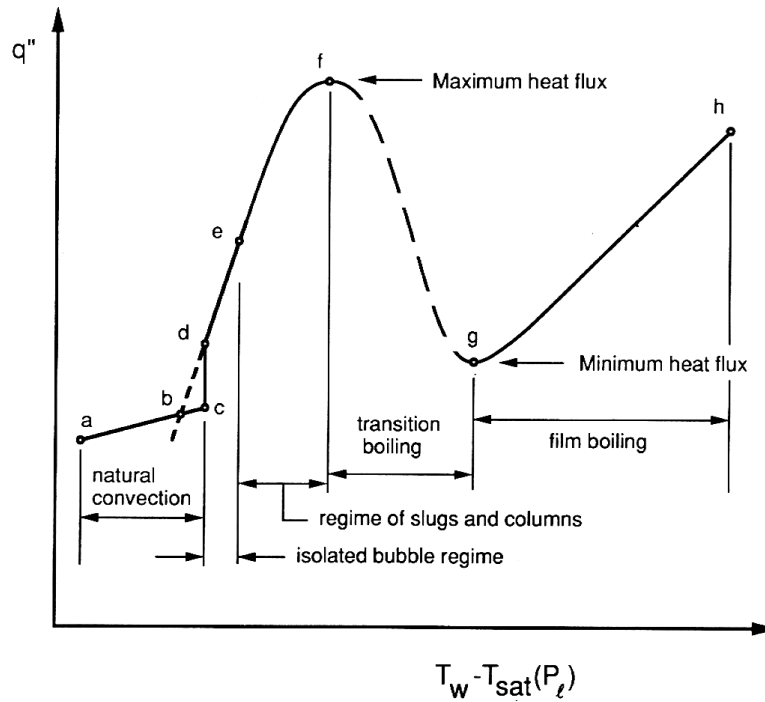


Figure 1.1: Boiling curve [2].

1.2 Introduction of Interaction

Particular discussions of isothermal and boiling systems are mentioned in each chapter.

A conceptual sketches of actual boiling surface was illustrated in Fig. 1.3.

Some theoretical studies have discussed only single bubble behaviors for several decades while collections of correlations have governed the boiling research field. Some recent experimental researches revealed that chaos rules in bubbling of boiling and isothermal system and it results from interaction between bubbles [6].

As already stated, the scopes of conventional boiling researches have been an average properties of whole surface. The reason why such approach have been taken is that an actual surface has randomly distributed nucleation sites which play the nucleation of vapor bubble and it is difficult to extract the fundamental process like single site dynamics. A recent micro-fabrication technology enables us to pick up the single bubble behavior. Takagi et al. [7] investigate experimentally and theoretically a behavior of a boiling bubble from a micro-scale heater. They evaluate fractions of heat quantity released

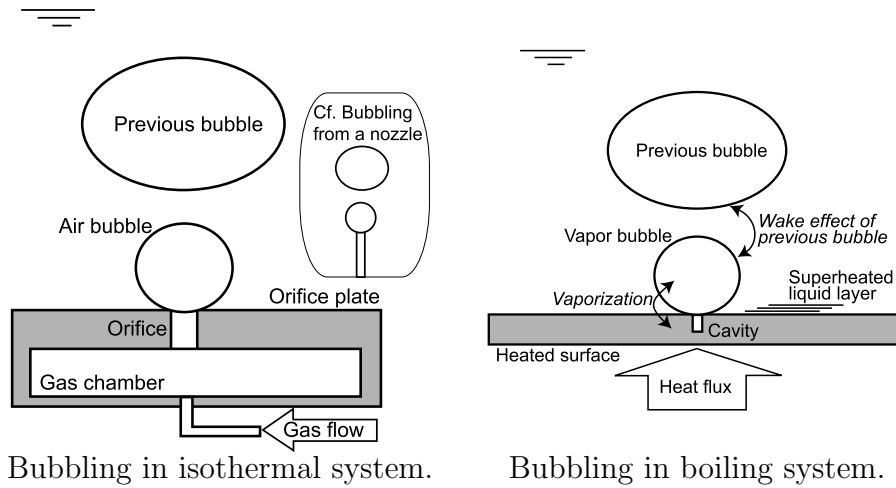


Figure 1.2: Analogy of bubbling between isothermal system and boiling system.

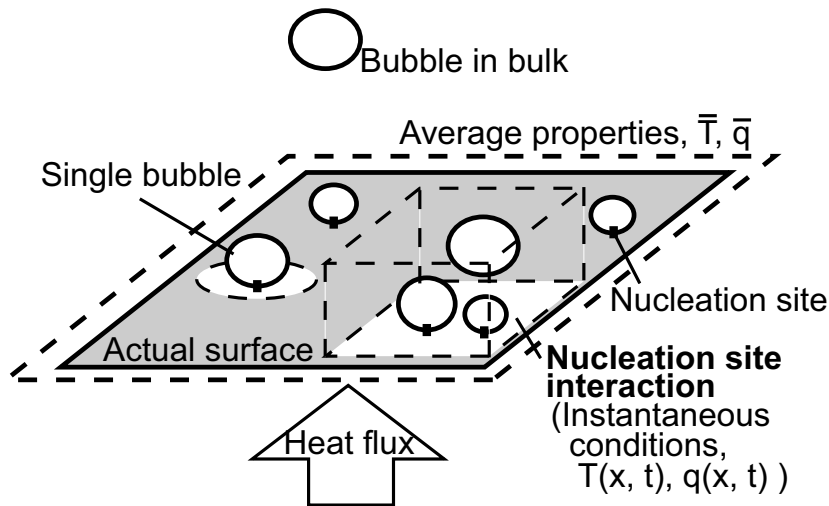


Figure 1.3: Actual boiling surface and interaction.

through different paths: vaporization, induced flow and natural convection. In contrast, many researches of isothermal system have studied bubble dynamics in bulk liquid. Heat transfer from heated surface, however, is influenced by a great deal by bubble behavior near the surface. This evidence is helpful to construct model in chapter 3 since we can consider small volume near the surface.

The analogy described in last section can be extended to bubble-bubble

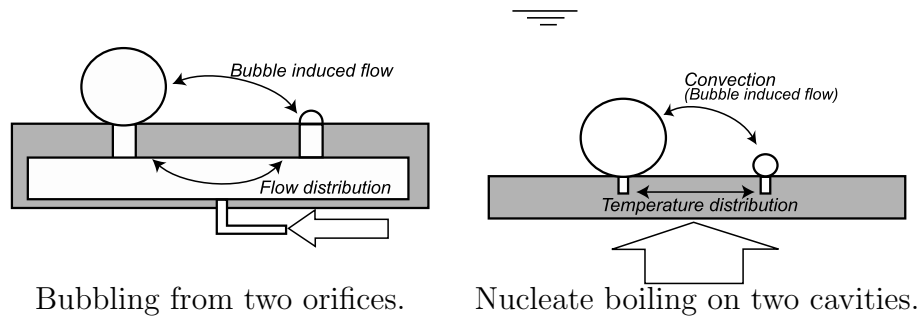


Figure 1.4: Analogy of bubble-bubble interactions between isothermal system and boiling system.

interaction. Isothermal system and boiling system with two bubbling sources are sketched in Fig. 1.4. Pressure of a chamber and superheat of heated surface drive the bubbling in isothermal and boiling system, respectively. Distributions of gas flow or heat flux cause interactions.

The difference, however, was pointed out by considering the governing equations of two systems. Hydrodynamical interaction was governed by equations of motions of liquid and gas which define second time derivatives of the quantities and remind us a concept of “inertia”. In contrast, Thermal interaction, a conduction, was governed by diffusion equations which determine first time derivatives of quantities.

1.3 Dynamical Behavior of Boiling

Hardenberg [8] et al. investigated experimentally the dynamics of boiling, especially nucleation site interaction using statistical analysis.

Numerical simulation of boiling is still unrevealed field due to interfacial phenomena. For example, discontinuity of interface structure, namely vapor bubble coalescence, and vaporization coefficient have been ambiguous yet. One of few researches, a study by Dhir [9], solved the conservation equation of mass, momentum and energy for the liquid and vapor phase simultaneously with the continuously evolving of the interface at and near a heated surface. The simulation results of the bubble behaviors showed good agreement with the experimental data. In this simulation, however, the temperature of heated surface was assumed to be constant.

There are few dynamical model of boiling as follows. Yanagita [10] employed coupled map lattice (CML, see an overview of CML by Kaneko [11]) to simulate boiling regimes, nucleate boiling and film boiling as shown in

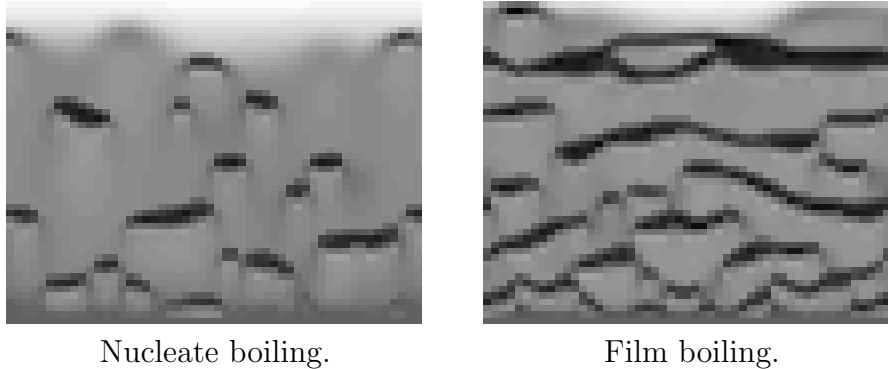


Figure 1.5: Coupled map lattice of boiling [10]. (These figures were reconstructed by the author).

Fig. 1.5. There is large degrees of freedom, number of meshes. The mesh was heated from below and cooled from top Darkness mean temperature and lamb of black lattices meaning bubbles feel buoyancy. It is a dynamical system with continuous field variables but with discrete space and time. It reproduce transition between nucleate boiling and film boiling by setting only several simple rules, conduction and buoyancy.

In contrast, Ellepola and Kenning [12] proposed a simplified dynamical model of an interaction between two nucleation sites only with three degrees of freedom, temperatures of two sites and an intervening wall. The time evolution of the model was based on conduction between each site and intervening wall, vaporization from each site and convective heat transfer from intervening wall. They illustrated that time series of temperature became chaotic or periodic depending on input heat flux. In this model, chaos comes from switching of vaporization (see the detail in his Ph.D thesis [13]).

1.4 Past Researches of Artificial Surface in Our Laboratory

Researches of nucleate boiling on artificial surface in our laboratory have started with boiling from a single cavity [14] by Shoji and Takagi. They examined the effects of cavity shapes: conical, cylindrical and reentrant. Yasui and Yokota performed the experiments in various conditions of diameters and depths of a cavity and a spacing between cavities (reviewed in Shoji [15]). Zhang and Shoji compiled these experiments and evaluated the interaction as reviewed in section 3.3. Surapong [16] performed the experiments of triple

cavities and analysis as Zhang and Shoji.

1.5 Objectives

There are models of two types: models for prediction and models for understanding. Numerical simulations and empirical correlations belong to the former. While they are very effective in engineering, they cannot grow our understanding well sometimes, especially for dynamical phenomena or interactions, even though they reproduce some curious experimental results.

In this master's thesis, the author proposed two simplified dynamical models for understandings of bubble-bubble interactions in isothermal and boiling systems. "Simplified" means number of variables, degrees of freedom, is not large and each variables are physically meaningful. These models were constructed in the form of deterministic dynamical systems, $\dot{\mathbf{x}} = \mathbf{f}(\mathbf{x})$, like a Lorenz model [17] which is simplified model of two dimensional Navier-Stokes equation under the condition as benard convection and behaves non-periodically only with three variables.

In chapter 2, bubbling from submerged twin orifices with a common plenum was dealt with. When the plenum volume is relatively small and a flow rate was extremely low, the bubbling from two orifices strongly interacts each other. Observation of bubbling and measurement of flow induced by bubble was conduct experimentally. A simplified mathematical model which describe time evolution of bubbles volumes is proposed and it reveals the mechanism of bubble-bubble interaction.

Taking a liking for results in isothermal system, the author attempt to construct a dynamical model of boiling bubble behavior on artificial surface and their interaction in chapter 3. As mentioned in subsection 1.2, interaction in boiling system become more difficult than isothermal system. Therefore more degrees of freedom is needed and it is ambiguous to understand even qualitatively.

Chapter 2

Interaction in Isothermal System

2.1 Introduction

Bubble formation has been widely used in industry such as chemical plants, bubble towers and the like. It is also an important physical process in boiling phenomena. To achieve a better comprehension about the bubble dynamics, numerous researches have been attempted in the past by focusing on bubble generation, growth and detachment (e.g., Clift et al. [18]). Most researches have had target on a single isolated bubble because the interaction between successively generated bubbles or adjacent bubbles is rather complex and difficult to deal with due to its strongly nonlinear nature. Thus the interactive aspects have been excluded from the consideration for long period by taking the average in time or in space. In many actual systems of utilizing bubbles, however, it is usual for multiple bubbles to appear. So the bubble-bubble interaction as well as bubble-liquid interaction is the essential issue, and some recent researches deal with such problem.

In a system of air bubble generation from a single nozzle in water, Mittoni et al. [19] and Tritton and Egdell [20] obtained time series of pressure signals at upstream nozzle or flow velocities near the nozzle exit. Then they carried out nonlinear analysis for the data, showing that some chaotic dynamics exists in the system. Shoji [21] observed period doubling bifurcation in departing bubble frequency of a chain of air bubbles generated from a single orifice submerged in water, and Zhang and Shoji [22] succeeded to explain the phenomena by proposing a nonlinear model which considers the interactive effects of the preceding bubble. In contrast, there are only a few researches available for the systems of multiple orifices. Titomanlio et al. [23]

conducted an experiment of bubbling from two orifices connected to a common chamber, and found that at high air flow rate, the detachment bubble volume is almost equal to that of a single orifice system having a half chamber volume in half flow rate. In a similar system, Ruzicka et al. [24] measured the pressure signal inside the chamber and found that the signal shows two different fluctuation structures “synchronous” and “asynchronous”, depending on the air flow rate. They also discussed nonlinear characteristics and its dependence on various control parameters. To our knowledge, there is no available model or theoretical approach to comprehend the interaction between bubble and bubble or between bubble and liquid.

This chapter describes the results of experimental and theoretical study performed to understand bubbling behaviors from submerged twin orifices that interact each other through a common chamber. In the experiment, bubbling feature was precisely specified varying gas flow rate. It is found that at relatively low flow rate, various bubbling patterns appear repeatedly in a complex manner. To reveal the mechanism of such pattern appearance and transition, a simplified theoretical model is proposed. This model describes the time evolution of bubble volume at each orifice basing on equation of motion for liquid and gas, which explains well the experimental results.

2.2 Experimental Apparatus

Fig. 2.1 shows the experimental apparatus schematically. Air and pure water were used as the test fluids. The air was supplied to the chamber under a constant flow rate by a compressor through a flow meter and a fine brass capillary tube of 0.3mm in inner diameter and 137mm in length. The capillary tube was served to maintain a constant flow rate condition. Bubbles were generated into a stagnant water pool from two cylindrical orifices of 2mm in diameter. The orifices were fabricated on a 1mm-thick, 60mm-diameter brass plate, which constitutes the top side-wall of the chamber.

The spacing between orifices plays an essential role in the effectiveness of interaction between generated bubbles. In general, the interaction involves two interactive processes: one through the liquid and the other through the chamber. In this study, in order to simplify the system, the spacing between orifices was taken large enough to be able to ignore the effects of interaction through liquid. Namely, attention was paid only to the interaction through the common chamber. According to the past researches of nucleate boiling (e.g., Calka and Judd [25] and Zhang and Shoji [26]), the interaction between horizontally-adjacent bubbles is negligible when the spacing between the nucleation sites is larger than three times of the bubble departure diameter. The

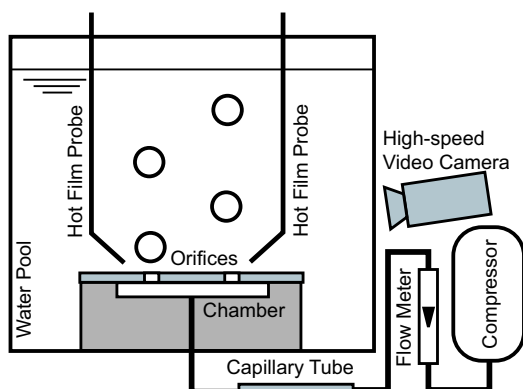


Figure 2.1: Sketch of experimental setups

critical spacing of this becomes 15mm in the present experiment because the bubble departure diameter was mostly around 5mm. So the spacing of 30mm employed in the present experiment is well expected to satisfy the condition, including a surplus. In the experiment, the chamber volume, V_c as well as the gas flow rate, q , was varied in a wide range. The following discussion, however, is restricted within a condition of $V_c = 10\text{ml}$ which the interaction become vivid.

Bubbling behaviors were observed by a high speed video camera with 1000 frames/s. A hot film probe was set at the vicinity of each orifice to detect liquid flow (micro convection) induced by generated bubbles. The location of the probe was 0.5mm height from the orifice plate and 3mm horizontal distance from the orifice center, which was determined from repeated preliminary tests to obtain maximum signal and to correspond well to the bubble generation, growth and departure. Thus the signal output becomes a good indicator of bubbling features, providing valuable information to diagnose the linearity or complexity of bubble generation and interaction.

2.3 Experimental Results

2.3.1 Bubbling pattern at low flow rate

In the present experiment, various types of bubbling patterns were observed, depending on the chamber volume as well as the air flow rate. Three types of bubbling patterns appear at relatively low flow rate. For each typical cases, the snapshot in Fig. 2.2 and time series of bubble volumes in Fig 2.3 are obtained from high speed movies, and the power spectrum calculated from

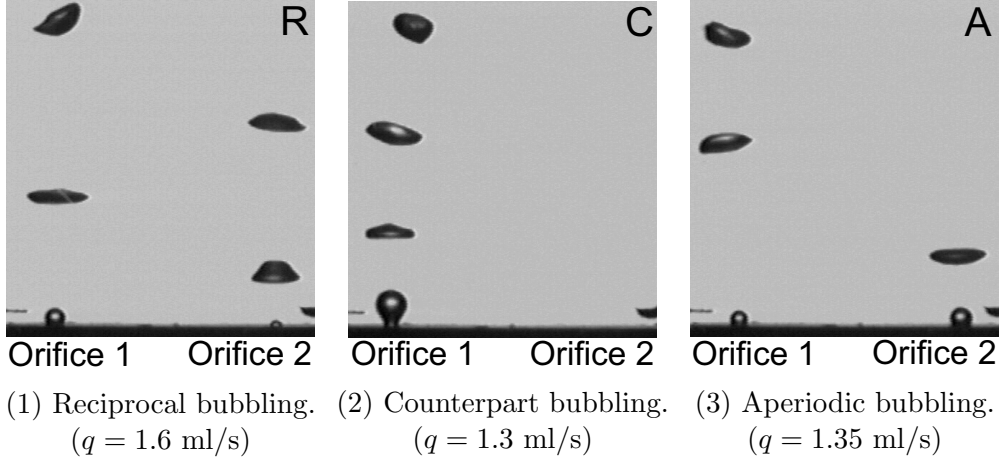


Figure 2.2: Snapshots of major bubbling patterns.

the signal of hot wire probe.

1 (Reciprocal bubbling) Bubbles are generated from each orifice reciprocally (Fig. 2.2–(1)). Once a bubble departs from the one orifice, the next bubble is generated and departs from the other orifice. Since the air may be supplied evenly in time to both orifice, fundamental frequency of bubble departure in this case becomes $f = q/2\bar{V}_d$, where \bar{V}_d is the averaged departure bubble volume (Fig. 2.3–(1)).

2 (Counterpart bubbling) Bubbles are generated from either of the orifices (Fig. 2.2–(2)). So the fundamental frequency in this case is $f = q/\bar{V}_d$, which is twice as large as that of reciprocal bubbling (Fig. 2.3–(2)).

3 (Aperiodic bubbling) This pattern does not belong to neither of the two patterns above mentioned (Fig. 2.2–(3)). Namely, several bubbles subsequently generate from either of the orifices but the active orifice changes from one to the other in a random manner (Fig. 2.3–(3)).

In any of the above-mentioned three patterns, bubbles synchronously start to grow from both orifices at the first stage of bubble generation. However, at the moment when the bubbles reach to a certain critical size, one bubble continues to grow while the other bubble stop to grow and diminishes to finally disappear.

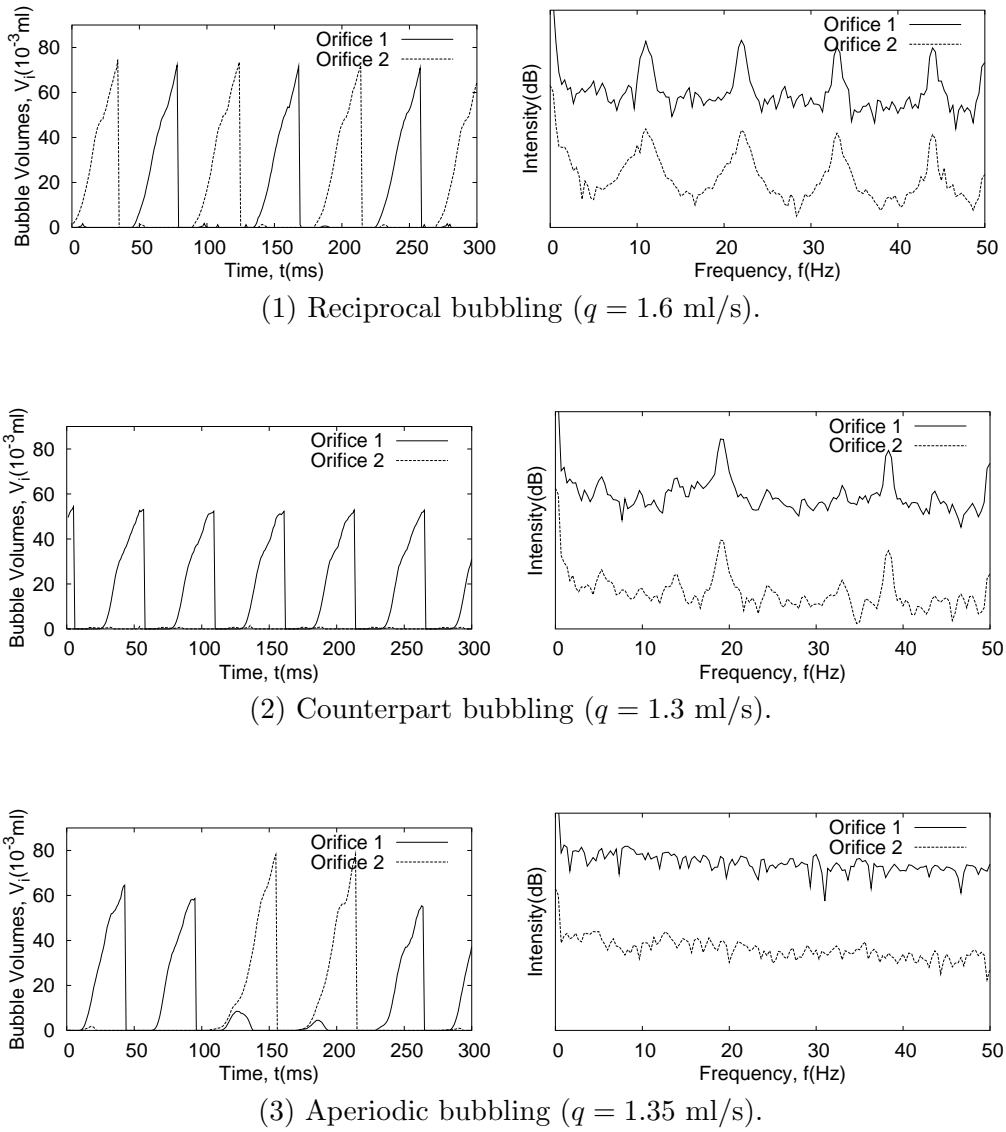


Figure 2.3: Time series of bubble volume and power spectrum of each bubbling pattern.

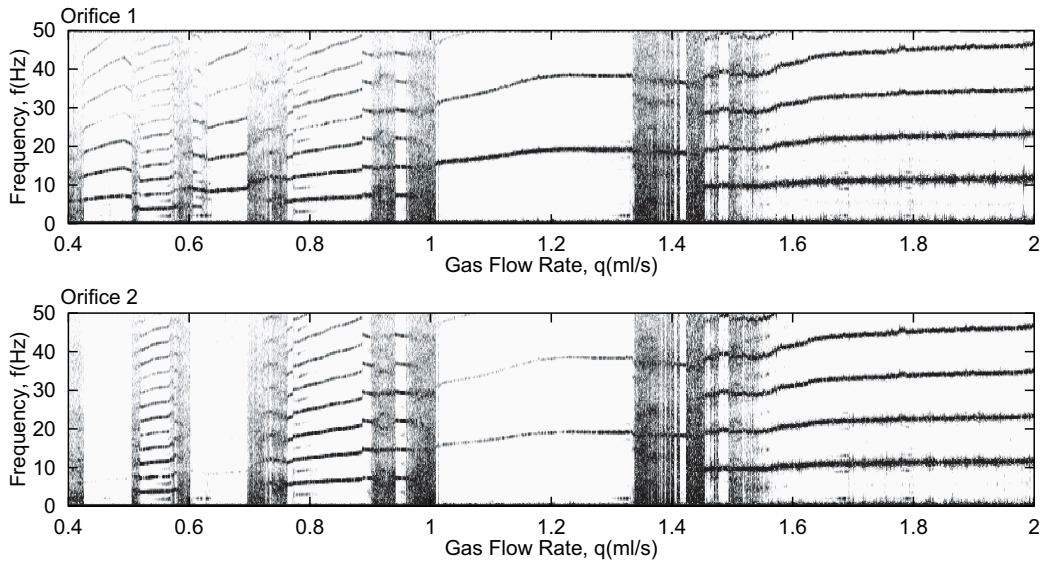


Figure 2.4: Spectrogram of wire probe signal.

2.3.2 Pattern transition

To obtain better matching between the air flow rate and the bubbling patterns and also to observe precisely the transition from one pattern to the other, the special test was conducted by gradually decreasing the air flow rate. This was a transient experiment but the decreasing rate of air flow was very slow at an order less than 0.01ml/s , so it may be said that the data obtained were of quasi steady state. Fig. 2.4 shows the spectrograms obtained from the hot wire probe signal of each orifice, in which the strength of the power (scale of the amplitude) of Fourier analysis is illustrated in colored for every signal-detected flow rate.

The region of air flow rates where clear peaks of frequency appear at both orifices corresponds to the periodic bubbling, and the region with no clear peaks to “aperiodic” bubbling. In the region of “counterpart” bubbling, a stripe appears only at an active orifice whereas in the region of “reciprocal” bubbling, stripes appear in both spectrograms for the two orifices. The fundamental frequency (i.e. the lowest peak) of “reciprocal” bubbling is lower than that of “counterpart” bubbling because the air flow is splitted to both orifice in time-average sense. The most interesting and important information that Fig. 2.4 provides is that a set of regions of air flow rate, where the two periodical patterns appear and aperiodic pattern exists in between, appear repeatedly in a wide range of air flow rate.

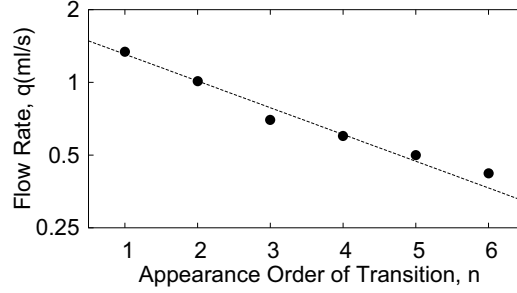


Figure 2.5: Flowrate at pattern transition(experiment).

2.3.3 Power law for pattern transition

The values of air flow rate, $q_{c,n}$, at which the set of the combined pattern region appears are plotted in Fig. 2.5 as a function of the order of the appearance, n . The data is well correlated by the following equation:

$$q_{c,n} = 1.68 \exp(-0.255n) \quad (2.1)$$

This result clearly indicates the existence of a power law, suggesting that some nonlinear chaotic dynamics exists in this system.

2.4 Simplified Theoretical Model

2.4.1 Assumptions

In order to reveal the physical mechanisms of bubbling features described in the previous section, especially the appearance, transition and repetition of bubbling patterns, a simplified model is constructed to describe bubble generation at each orifice. In this modeling, bubble volume at each orifice, V_1 and V_2 , are taken as a couple of variables, and the local pressure at the inlet of each orifice is considered. The fluctuation of the pressure connects to the instantaneous variation of each variable (each bubble volume). The main issue concerned here is to make clear the physical process how the distribution of air supplied into two orifices is determined and why it becomes uneven, which may finally yield complex bubbling features. Since the present system is symmetry with respect to two orifices, the governing equations of the model should be written in the form as

$$\begin{cases} \ddot{V}_1 = f(V_1, V_2, \dot{V}_1, \dot{V}_2; q) \\ \ddot{V}_2 = f(V_2, V_1, \dot{V}_2, \dot{V}_1; q). \end{cases} \quad (2.2)$$

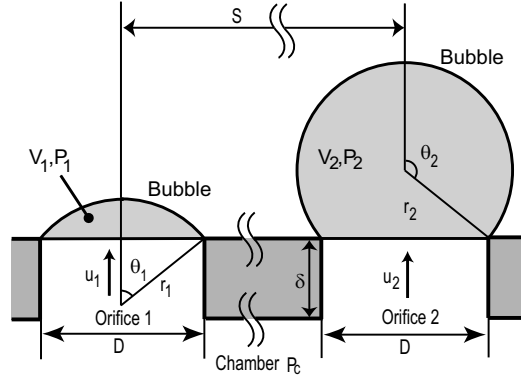


Figure 2.6: Sketch and notation of idealized bubble shape

Here q is the volumetric air flow rate supplied into the chamber. In the present model, q is a parameter but is considered to be constant in time.

For simplicity, the followings are assumed:

Assumption 2.1 The bubble shape is a sectional part of a sphere as shown in Fig. 2.6. So the instantaneous bubble volume and radius of curvature of the bubble are respectively expressed as follows:

$$V_i(r_i) = \frac{\pi r_i^3}{3} (\cos^3 \theta_i - 3 \cos \theta_i + 2) \quad (2.3)$$

$$r_i = \frac{D}{2 \sin \theta_i}. \quad (2.4)$$

Assumption 2.2 Properties of air and water are constant. This assumption includes the incompressibility of air as well as water.

Assumption 2.3 The viscous effects of liquid motion are negligible.

Assumption 2.4 The inertia effects of gas flow in bubble growth are negligible.

Assumption 2.5 The bubble departure volume is determined from the force balance between buoyancy and surface tension as follows:

$$V_d = \frac{\sigma \pi D}{(\rho_\ell - \rho_g)g}. \quad (2.5)$$

After the bubble departs from the orifice with the value of Eq.(5), the next following bubble is assumed to start growing from zero volume. This assumption is a nonlinear on-off condition but it is noted that the continuity of variables and that of its time derivative hold except the volume at the instant of detachment.

Assumption 2.6 The volumetric air flow rate into the chamber is constant. This assumption together with Assumption 2.2 indicates that the total air flow rate supplied to the twin orifices is constant. This condition can be written in the following forms:

$$\dot{V}_1 + \dot{V}_2 = q \text{ (Const.)} \quad (2.6)$$

$$\ddot{V}_1 + \ddot{V}_2 = f_1 + f_2 = 0. \quad (2.7)$$

The interaction between bubbles generated from two orifices is restricted by the conditions of Eqs.(2.6) and (2.7).

Assumption 2.7 There is no pressure drop inside the passage of the orifice. In general, equation of motion of gas inside the orifice can be written as

$$\frac{\partial u_i}{\partial t} = -\frac{1}{\rho_g} \frac{\partial P}{\partial x} - u_i \frac{\partial u_i}{\partial x} + \nu_g \frac{\partial^2 u_i}{\partial x^2} \quad (i = 1, 2). \quad (2.8)$$

By integrating Eq.(2.8) with respect to x (flow direction), the Assumption 2.3 yields

$$\delta \frac{\partial u_i}{\partial t} = \frac{1}{\rho_g} (P_c - P_i) \quad (i = 1, 2). \quad (2.9)$$

Noting that $Au_i = \dot{V}_i$, Eq.(2.9) can be rewritten for the bubble volume as

$$\ddot{V}_i = \frac{A}{\rho_g \delta} (P_c - P_i) \quad (i = 1, 2). \quad (2.10)$$

2.4.2 Phenomenological governing equations

In order to complete the model formulation, instantaneous pressure inside the growing bubble must be considered. As well known as the Rayleigh-Plesset equation (e.g. Plesset and Prosperetti [27]), the equation of motion of liquid around a spherical bubble is given by

$$P = \frac{2\sigma}{r} + \rho_\ell (r\ddot{r} + \frac{3}{2}\dot{r}^2) + \frac{4\mu_\ell}{r}\dot{r}. \quad (2.11)$$

Here, P is the excess pressure from that of liquid far from the bubble. The terms of right hand side of Eq.(2.11) represent surface tension, inertial force

and viscous force, respectively. Laplace pressure is often used for measurement of surface tension [28]¹. If we rewrite Eq.(2.11) by taking the bubble volume as the variable in place of r , we can learn with ease that inertial and viscous terms in Eq.(2.11) relate to \dot{V}^2 and \dot{V} respectively. So from Eq.(2.11) together with the Assumption 2.1, the pressure inside the bubble may approximately be expressed in the following form:

$$P_i = \frac{2\sigma}{r_i} + \beta\dot{V}_i^2 \quad (i = 1, 2). \quad (2.12)$$

In deriving Eq.(2.12), it is assumed that the coefficient of inertia term, β , is constant. By substituting Eq.(2.12) into Eq.(2.10) and by eliminating P_c using the relation of Eq.(2.7), the following set of governing equations are obtained:

$$\begin{cases} \ddot{V}_1 = \frac{A}{2\rho_g\delta}(P_2 - P_1) \\ \ddot{V}_2 = \frac{A}{2\rho_g\delta}(P_1 - P_2), \end{cases} \quad (2.13)$$

where

$$P_i = \frac{2\sigma}{r_i} + \beta\dot{V}_i^2 \quad (i = 1, 2). \quad (2.14)$$

2.5 Model Behavior

Basing on the present model, the simulation was performed using the governing equations of Eqs.(2.13) and (2.14). The constants involved in the equations are $A/(\rho_g\delta) = 9.52 \times 10^{-5}$ and $\beta = 5 \times 10^{11}$ for the present experimental conditions.

2.5.1 Configuration space and phase space

Configuration space is a mathematical space easy to discuss the dynamic behaviors of a physical system. The configuration space of the present case can be constructed by taking bubble volumes, V_1 and V_2 , as coordinates. On this space, an instantaneous state of the twin bubbles is expressed by the point (V_1, V_2) , and the time evolution of the state by the movement (trajectory) of the point. The trajectory is determined by Eq.(2.13). A typical example of the trajectory is shown in Fig. 2.7 by a thin solid curve, which indicates the bubble volume time-development starting from a certain

¹Few people are aware that one of its pioneers was a young physicist named Erwin Schrödinger, back in 1915

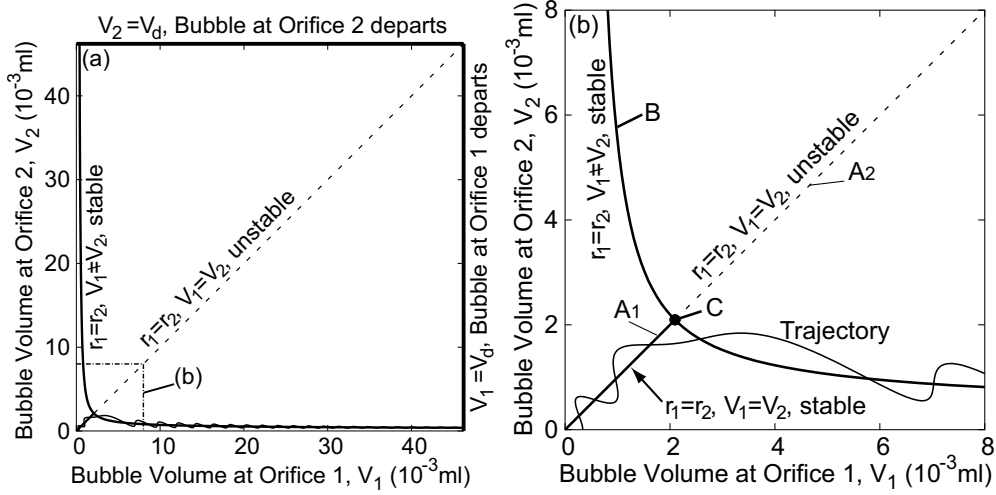


Figure 2.7: A typical example of trajectory on configuration space.

initial condition under the air flow rate of $q = 1.0 \text{ ml/s}$. Since the total air flow rate supplied to the twin orifices is constant (Assumption-2.6), the point on the trajectory moves at a constant speed in the upper-right direction while at the velocity determined by Eqs.(2.13) and (2.14) in the upper-left direction. The time variation of bubbles state is much easily understand on phase space. As the total air flow rate supplied to the twin orifices, $\dot{V}_1 + \dot{V}_2$, is constant (Assumption-2.6), the phase space can be constructed in three dimensional space by taking V_1 , V_2 and \dot{V}_1 as the coordinates. Fig. 2.8 shows the trajectory of Fig. 2.7 on this space.

2.5.2 Effect of surface tension

At low flow rates, the surface tension plays a significant role. The excess pressure due to surface tension, the surface tension term in Eq.(2.14), changes with bubble volume as is shown in Fig.2.9. When the bubble shape is hemispherical, the radius of curvature becomes minimum, at which the excess pressure takes the highest value. The line A (A1 and A2) and the curve B on the configuration space represent the curves when the twin bubbles grow with the same curvature and the same volume (A:A1, A2) and with the same curvature but the different volume (B), respectively, for an extreme case of dominant surface tension effects. As for line A, the part of solid line, A1, and the part of dotted line, A2, are the stable and unstable region, respectively.

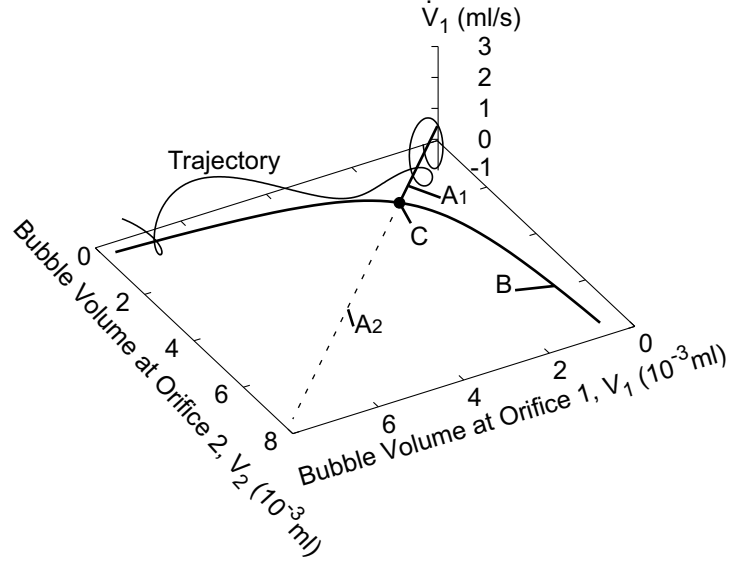


Figure 2.8: A typical example of trajectory on phase space.

The stability condition is

$$\frac{\partial^2(1/r_1 - 1/r_2)}{\partial(V_1 - V_2)^2} > 0. \quad (2.15)$$

The neutral point, C, is $(\pi D^3/12, \pi D^3/12)$. It is noted that the part of A2 becomes stable at high air flow rates where the inertia of air flow dominant and surface tension effect is negligible. When the surface tension effect is dominant, only one bubble departs from either of the two orifices. Namely, twin bubbles grow simultaneously with the same volume, along the line A2 until the point, C, on the configuration space. However, at the point C, bifurcation takes place, and then, one bubble continues to grow whereas the other bubble diminishes its volume to finally disappear, along the curve B.

2.5.3 Effect of inertial force

When the inertial term is dominant and surface tension effects is negligible, Eq.(2.13) takes the form as

$$\begin{aligned} \ddot{V}_1 - \ddot{V}_2 &= 2 \frac{A\beta}{2\rho_g \delta} (\dot{V}_2^2 - \dot{V}_1^2) \\ &= -\frac{A\beta q}{\rho_g \delta} (\dot{V}_1 - \dot{V}_2), \end{aligned} \quad (2.16)$$

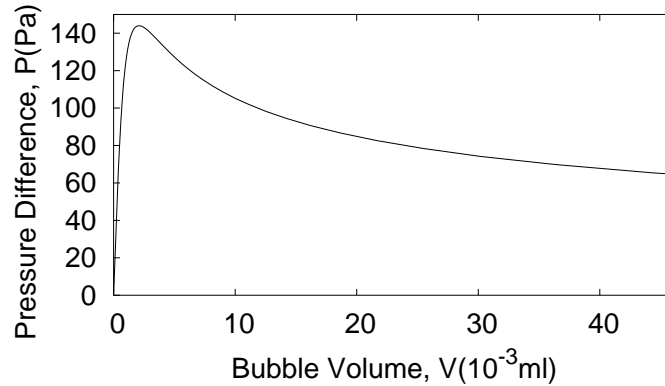


Figure 2.9: Pressure difference with surface tension.

where $A\beta q/\rho_g\delta > 0$. Equation (2.16) indicates that the inertial term has the effect of attenuating the fluctuation of bubble volume. The fluctuation is generally induced by surface tension effects.

2.5.4 Growth of twin bubbles and trajectory on configuration space

Both effects of surface tension and liquid inertia determine the bubble growth and departure, which yield three bubbling patterns. The typical examples of bubble volume time series and bubble growth trajectories on phase spaces are shown in Fig. 2.10 for the three patterns, corresponding to three different air flow rates.

The physical mechanisms how the three patterns appear may be clear if the set of initial condition for bubble generation is considered on the planes of $V_1 = 0$ and $V_2 = 0$ in phase space. The condition at bubble detachment is given as a point on the plane of $V_1 = V_d$ or $V_2 = V_d$ in the phase space. Once the bubble departs, the point is transferred to the the plane of $V_1 = 0$ or $V_2 = 0$. The set of such points divides each plane into two regions, one region where the bubble departs from same orifice and the other where it departs from the other orifice. When the initial condition of the following bubble returns to the same region of the same plane ($V_1 = 0$ or $V_2 = 0$) of the preceding bubble, the pattern becomes “counterpart”. When the initial condition return to the other region of the other plane, the pattern becomes

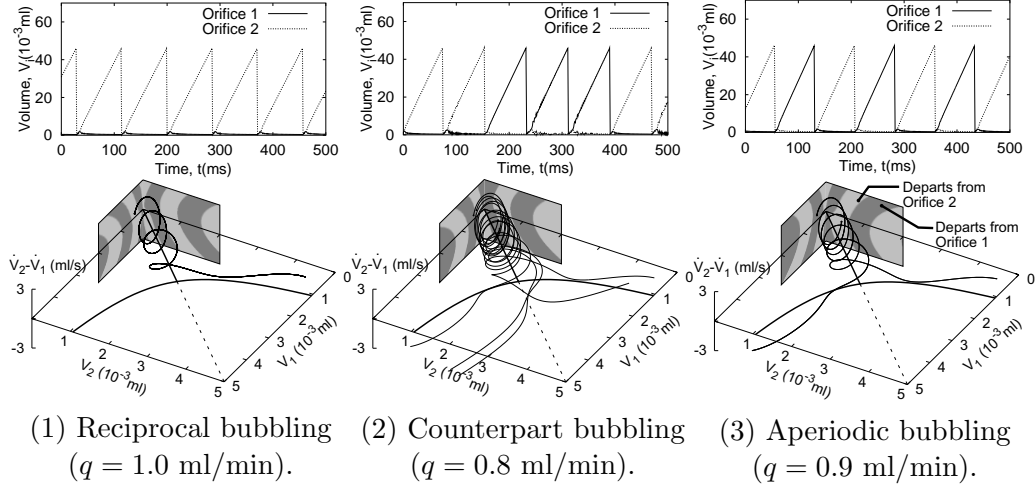


Figure 2.10: Time series of bubble volumes and phase space expression.

“reciprocal”. In other cases, the pattern becomes “aperiodic”. Divided region depends on flow rate.

2.5.5 Simulated spectrogram and power law

Fig. 2.11 and Fig. 2.12 are the simulated results for spectrogram and the power law, respectively, which should corresponded to experimental results of Fig. 2.4 and Fig. 2.5, respectively. Fig. 2.11 was constructed with time series of bubble volume. The agreement between simulation and the experiment are extremely good for both results. For example, the simulated results for the power law can be correlated by the following equation:

$$q_{c,n} = 2.02 \exp(-0.257n) \quad (2.17)$$

The exponent of Eq.(2.17) satisfactorily coincides with that of Eq.(2.1)

2.6 Concluding Remarks

To understand better the dynamic processes of bubbles generation and interaction, the experiment of bubbling from the submerged twin-orifices was performed in the air-water isothermal system, by varying widely the chamber volume and the volumetric air flow rate. Particularly under the condition of small chamber volume at relatively low flow rate, the features were able to be

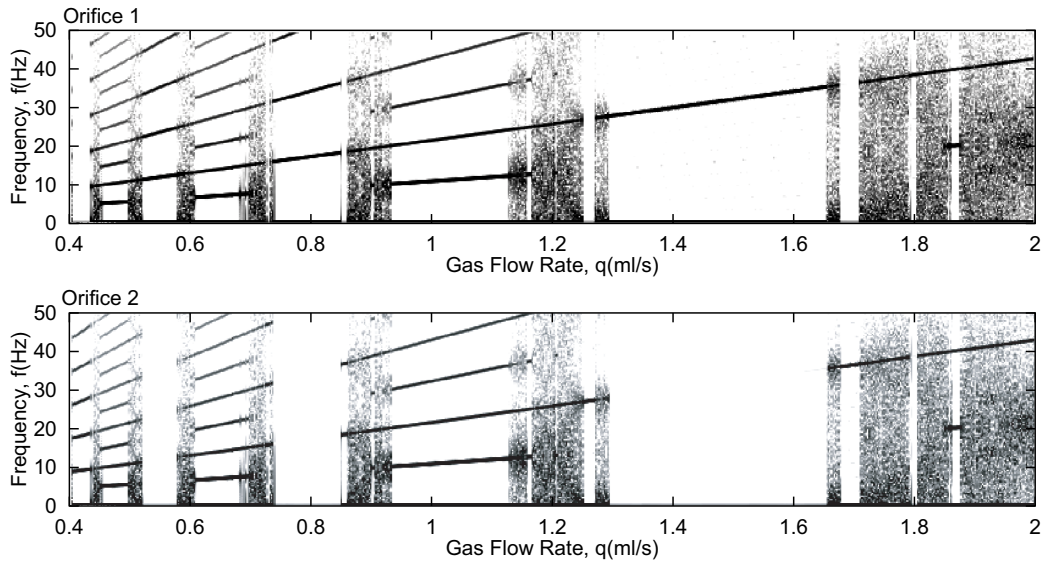


Figure 2.11: Spectrogram of simulation results against experimental results of Fig. 2.4.

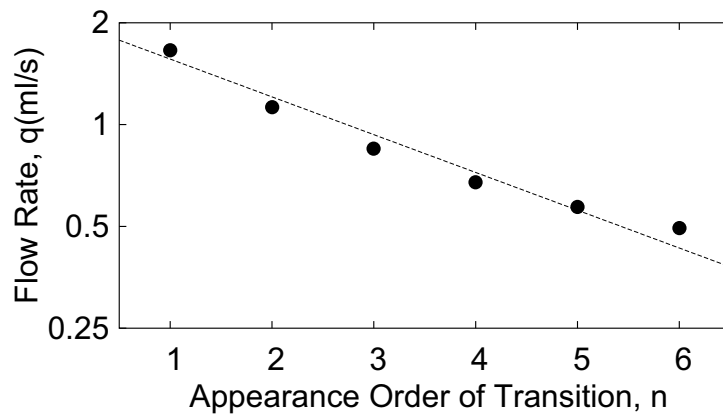


Figure 2.12: Flowrate at pattern transition of simulation results against experimental results of Fig. 2.5.

classified finely into three patterns of “reciprocal”, “counterpart” and “aperiodic”. With changing flow rate, the region involving those three patterns repeatedly appear. The data of air flow rate at which the pattern transition took place obeyed to a power law as a function of pattern appearance order, indicating that some nonlinear chaos dynamics exists in the present system. A simplified theoretical model was constructed to reveal the mechanism of bubble generation and interaction, which explain well the experimental results.

Chapter 3

Interaction in Boiling System

3.1 Introduction

In contrast with isothermal system, boiling system may need more variables to express the interaction since boiling is a phenomenon driven with hydrodynamics and thermodynamics while isothermal was driven with hydrodynamics. Bubble growth rates cannot be controlled explicitly in boiling system while in isothermal system was controlled by the gas flow rate. Additionally Calka and Judd [25] studied experimentally the distance of influence of to adjacent sites. They conclude that nucleation sites of 3 times of bubble diameter away, don't affect a behavior of the site. This experimental evidence indicates that it is meaningless to estrange two sites for reducing hydrodynamical interaction in liquid side by as done in last chapter.

Ellepola and Kenning [12] was an only theoretical research dealt with the interaction between nucleation sites to author's knowledge. Interaction of their model includes only conductive heat transfer between sites as following equations,

$$m_1 C_{p1} \dot{T}_1 = -R_{12}(T_1 - T_2) - \langle Q_{b1} \rangle + Q_{e1} \quad (3.1)$$

$$m_2 C_{p2} \dot{T}_2 = R_{12}(T_1 - T_2) - R_{23}(T_2 - T_3) - h(T_2)\Delta T_2 + Q_{e2} \quad (3.2)$$

$$m_3 C_{p3} \dot{T}_3 = R_{23}(T_2 - T_3) - \langle Q_{b3} \rangle + Q_{e3} \quad (3.3)$$

where $\langle Q_{b1} \rangle$ and $\langle Q_{b3} \rangle$ act only after T has reached the activation superheat but has not decreased to the deactivation superheat. Conductive heat transfer term ($R_{ij}(T_i - T_j)$) connects nucleation sites and makes two temperature close while heat flux term (Q_{ei}) rise and vaporization, $\langle Q_{b1} \rangle$ and $\langle Q_{b3} \rangle$, and convective heat transfer, $h(T_2)\Delta T_2$, fluctuate temperature of each part.

This chapter describes the results of experimental and theoretical study performed to understand bubbling behaviors from two artificial nucleation

sites (cavities) that interact each other through heated surface and superheated liquid. In the experiment, temperature fluctuation of each site and bubbling behavior was observed precisely. To reveal the mechanism of cavity spacing dependency of average bubbling frequency and periods distribution, a simplified theoretical model is proposed as in last chapter. This model describes the time evolution of bubble radius, surface temperature and previous bubbles' motion at each site.

3.2 Experimental Setups

Figure 3.1 sketches experimental system of nucleate pool boiling. A test chip with two artificial cavities (nucleation sites) was submerged in a vessel (water pool). The two cavities was fabricated with DRIE (Deep Reactive Ion Etching) method which can fabricate high aspect ratio hole due. A Cavity is 10 [μm] in diameter and 80 [μm] in depth and silicon plate is 200 [μm] of thickness. Spacing between cavities, S , was set 1–8 [mm] in water experiment and 0.3–6 [mm] in IPA. Auxiliary heater maintain bulk liquid temperature in the pool on saturated temperature. Distilled water or isopropanol(IPA) was used as test liquid. Vicinity of the manufactured cavities was heated by laser irradiation of 14 [mm] in diameter from the bottom of the plates.

Bubbling from sites was observed with a high-speed video camera. Sampling time of a frame is 1 [ms]. Surface temperature of the chip was simultaneously measured by a thermography. Sampling time of a frame is 3 [ms], the limit of the thermography ¹.

To our knowledge, both noncontact measurement and noncontact heating is unique while, in other pool boiling research, laser heating was used by Golobič and Gjerkeš [29] and infrared camera(thermography) and liquid crystal thermography was used by Theofanous et al. [30] and Kenning et al. [31], separately.

3.3 Experimental Results

3.3.1 Bubbling frequency[26]

Using this system, Zhang and Shoji [26] studied the interaction between nucleation sites and evaluated the effects of cavity spacing, S , on the interaction as average bubbling frequency (see open circles plotted in Fig. 3.2). They

¹As discussed later, it is not sufficient for tracking the bubble behavior.

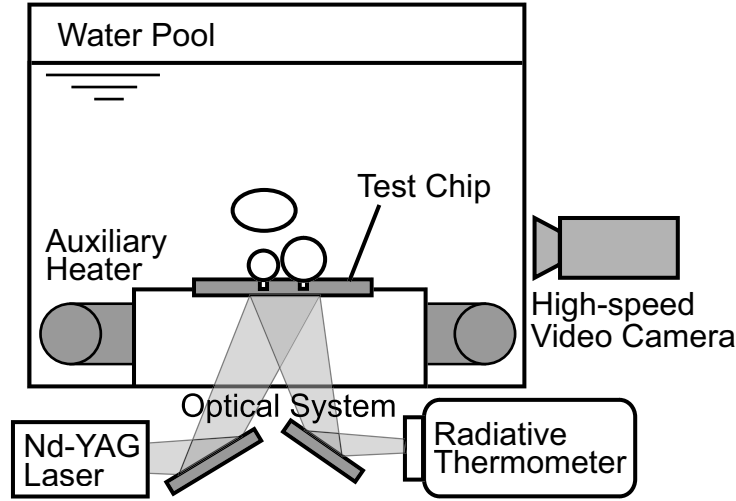


Figure 3.1: Schematic diagram of experimental system of nucleate pool boiling on artificial surface

separate the three factor: hydrodynamic interaction, thermal interaction and coalescence as summarized in Table. 3.1.

Mosdorf and Shoji [32] conduct a nonlinear analysis of this experimental data.

3.3.2 Distribution of bubbling periods

The experimental data of [26] was analyzed in detail and found that bubbling is less periodical (see distributed circles in Fig. 3.3). In all spacings, average bubbling frequency deviated slightly due to the departure of small bubble.

Table 3.1: Influence intensity of three effect factors of nucleation site interaction for different S/D ; +, - and \times mean the effect is frequency promotive, inhibitive and negligible

	$S/D \leq 1.5$	$1.5 \leq S/D \leq 2$	$2 \leq S/D \leq 3$	$3 \leq S/D$
Hydrodynamic interaction between bubbles	+	+	+	\times
Thermal interaction between nucleation sites	-	-	\times	\times
Horizontal and declining coalescence	+	\times	\times	\times

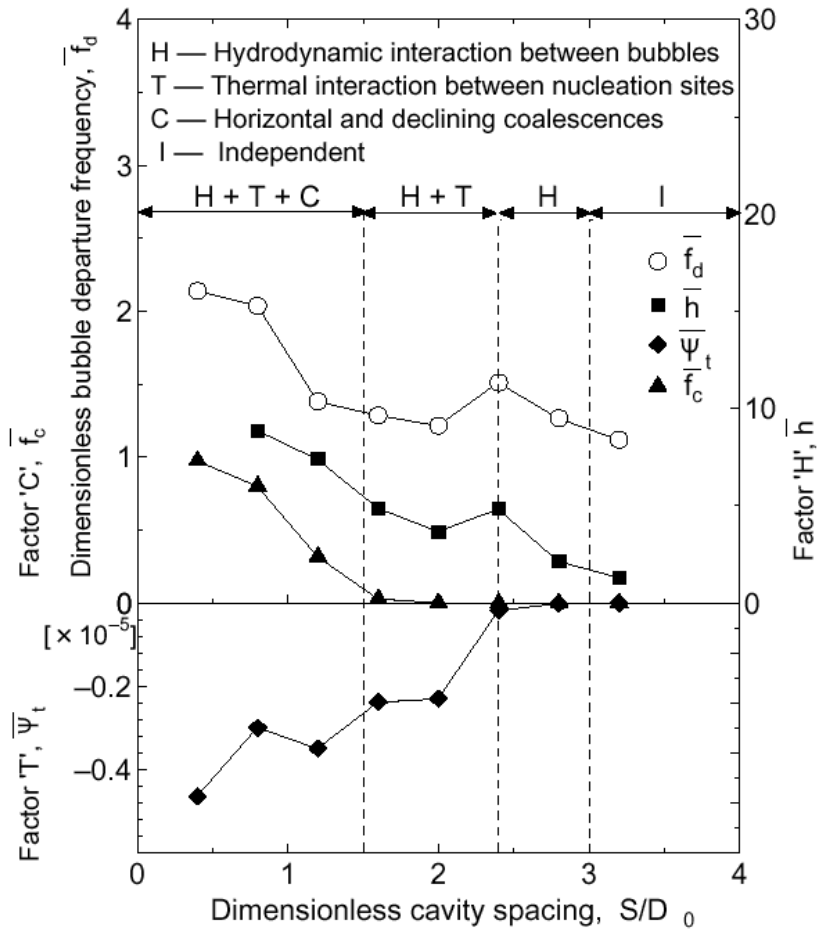


Figure 3.2: Bubbling frequency and three dominant factors

3.3.3 Photographic observation

Experimental results reveal that the bubble coalescence include two main kinds: coalescences far away from the surface and coalescences near the surface. Because the former one has very weak effect on the bubble growth and departure, the present research only focuses on the bubble coalescences near the surface. Through the observation of video, we find that the coalescences near the surface can also be further classified into three types: vertical coalescence, horizontal coalescence and declining coalescence (Shown in Figs. 3.4 to 3.6). Vertical coalescence means that during the growth process of the following bubble, it contacts with the previous bubble and then seems to be pulled away and absorbed by the previous bubble within an extreme short time period. In Fig. 3.4, the small following bubble on the left side is ab-

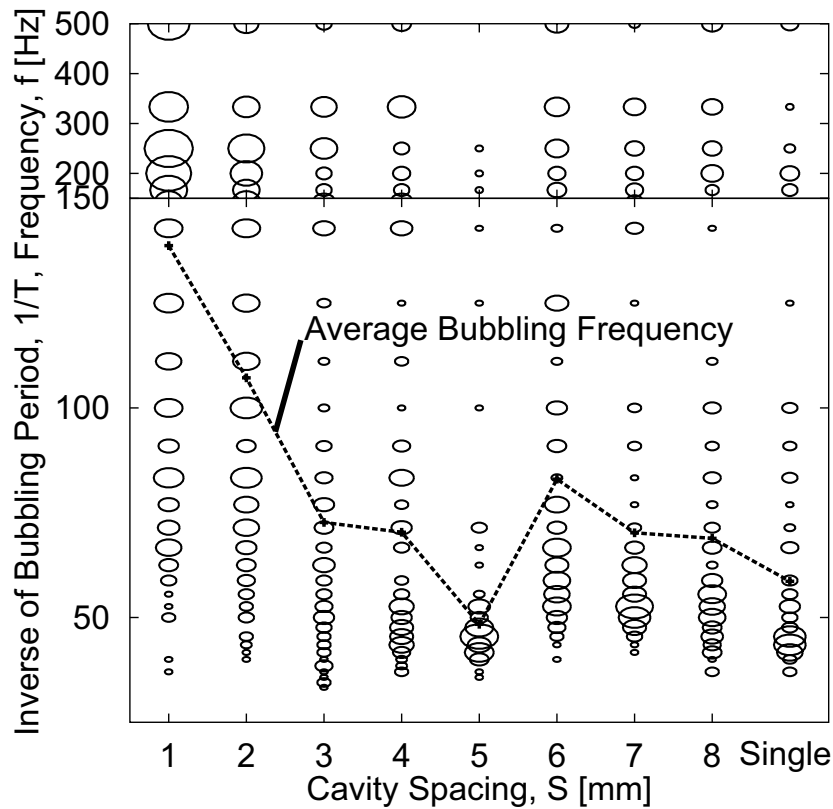


Figure 3.3: Bubbling period distribution (Experiment)

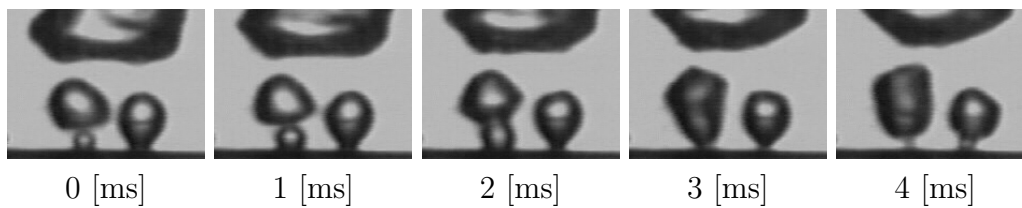


Figure 3.4: Vertical coalescence (at left site)

sorbed by its previous bubbles contact with each other and then coalesce into one bigger bubble. It seems that this coalesced bubble can reach force balance immediately through some deformation and then depart from the surface quickly (Katto and Yokoya [33] observed similar phenomena, small bubble pulling after large bubble detachment in nucleate boiling under high heat flux condition).

Declining coalescence can be detected between a growing bubble on a

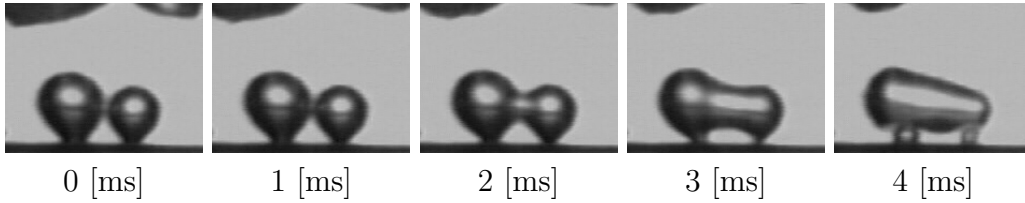


Figure 3.5: Horizontal coalescence.

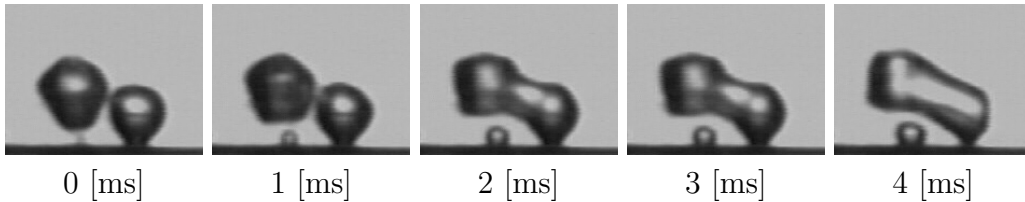


Figure 3.6: Declining coalescence (of preceding bubble at left site and bubble on right site)

nucleation site and a departed bubble over an adjacent nucleation site. In Fig. 3.6, the growing bubble on the right cavity contacts with the departed bubble instantly and a bigger coalesced bubble is formed. Through the vertical and the declining bubble coalescences, the buoyancy force of the coalesced bubble is distinctly increased while the inhibitive force are approximately unchanged. This is helpful for the present bubble to depart from the surface.

3.4 Simplified Theoretical Model

3.4.1 Problem statement

In isothermal system described at previous chapter, problem was stated only with hydrodynamical factors, momentum and surface tension. In boiling system, however, bubbling results from vaporization of superheated liquid layer and thermal factor must be included.

According to Zhang and Shoji [26], this model consists three part, thermal interaction, hydrodynamical interaction and coalescence.

In this section, we constructs a dynamical model of boiling bubble behavior. This model includes the effects conduction, convection and coalescence as simple as possible. Bubble growth rate was based on Mikic et al. [34].

Since the present system is symmetry with respect to two orifices, the

governing equations of the model should be written in the form as,

$$\dot{\mathbf{x}}_1 = \mathbf{f}(\mathbf{x}_1) + \mathbf{g}(\mathbf{x}_1, \mathbf{x}_2) \quad (3.4)$$

$$\dot{\mathbf{x}}_2 = \mathbf{f}(\mathbf{x}_2) + \mathbf{g}(\mathbf{x}_2, \mathbf{x}_1). \quad (3.5)$$

where $\mathbf{f}(\mathbf{x}_i)$ represents a self dynamics of single site i and $\mathbf{g}(\mathbf{x}_i, \mathbf{x}_j)$ is an interaction term which connects the two sites.

Pertinent variables must be chosen. Nucleate boiling is a consumption of superheated liquid layer. It is detected with bubble growth and surface temperature. In addition, a previous bubble strongly affects succeeding bubble. So it is assumed that following variables, \mathbf{x}_i , state an instantaneous condition of a single site as a minimum set.

$$\mathbf{x}_i = (r_i, T_i, y_{\text{pre}}) \quad (i = 1, 2) \quad (3.6)$$

These variables vary continuously while other variables, r_{pre} (radius of a previous bubble) is constant. All variables changed discontinuously when the bubble depart.

3.4.2 Assumptions

This modeling assumes following several assumptions. Here, notation of the model was taken as shown in Fig. 3.7.

Assumption 3.1 . The bubbles' shapes on heated surface and previous bubble are spherical.

The observation of experiment guaranteed this assumption in terms of bubbles on heated surface. A actual previous bubble were deformed to spherical cap by inertial effect of liquid, so this assumption is just for simplicity of coalescence calculation. Bubble volume and its time derivative is expressed with bubble radius as,

$$V = \frac{4\pi}{3} r^3 \quad (3.7)$$

$$\dot{V} = 4\pi r^2 \dot{r} \quad (3.8)$$

Generally, bubble behavior in bulk liquid few radius away from heat transfer surface don't affect strongly heat transfer in stagnant pool boiling. This model includes only bubbles attached on a surface, just previous bubbles and induced flow by them.

Assumption 3.2 Vertical velocity of detached bubble was constant. In the light of experiment evidence, a steady-rise velocity of the ascending

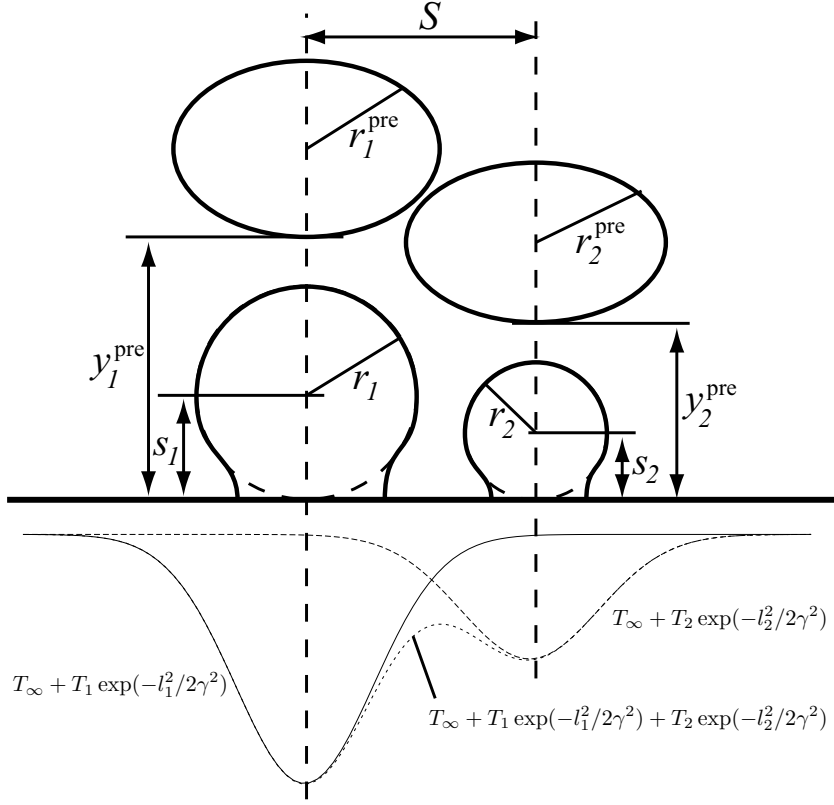


Figure 3.7: Notation of bubble condition

bubble in the calculation of its wake effect on the subsequent bubble seems to be valid. The velocity in the model was defined based on terminal velocities as following equations,

$$u_{\text{pre}} = \frac{2}{3} \sqrt{\frac{gr_{\text{pre}}(\rho_{\ell} - \rho_{\text{v}})}{\rho_{\ell}}} \quad (3.9)$$

or

$$u_{\text{pre}} = \frac{(\rho_{\ell} - \rho_{\text{v}})g}{3\rho_{\ell}\nu_{\ell}} r_{\text{pre}}^2. \quad (3.10)$$

Assumption 3.3 Heat diffusion drives bubble growth rate. Cole and Shulman [35] showed experiment results agree with the well known

bubble growth rate equation for $Ja < 100$ with and without dimension,

$$D = Ja\sqrt{\pi\alpha t} \quad (3.11)$$

$$\text{or } D^* = \sqrt{\pi}Ja \cdot Fo^{\frac{1}{2}} \quad (3.12)$$

Under the condition of constant surface temperature ², Eq.3.12 is differentiated with respect to time, Fo, as

$$\frac{dD^*}{dFo} = \frac{\sqrt{\pi}}{2}Ja \cdot Fo^{-\frac{1}{2}} \quad (3.13)$$

$$= \frac{\pi Ja^2}{2D^*}. \quad (3.14)$$

Eq. 3.14 does not include time explicitly. In other words, an instantaneous bubble radius determines its growth rate. Eq. 3.14 is expressed with radius, $r^* = D^*/2$ as

$$\frac{dr^*}{dFo} = \frac{\pi}{8}Ja^2 \frac{1}{r^*}. \quad (3.15)$$

Assumption 3.4 Bubble departs when the perpendicular distance between bubble center and surface, s , becomes larger than instantaneous radius, r , [36],

$$s(t) > r(t). \quad (3.16)$$

r grows according to assumption 3.3 while s grows whereby dynamical force balance between drag force and buoyancy force,

$$\frac{d}{dt}((\xi\rho_\ell + \rho_v)V\dot{s}) - f_{\text{wake}} = (\rho_\ell - \rho_v)Vg. \quad (3.17)$$

Here, ξ is 11/16 for bubble touched on plate. Equation of motion of s is obtained from Eq. 3.17 as,

$$\ddot{s} = \frac{1}{V} \left(\frac{f}{\xi\rho_\ell + \rho_v} - \dot{V}\dot{s} \right) \quad (3.18)$$

where

$$f = (\rho_\ell - \rho_v)Vg - f^{\text{wake}} \quad (3.19)$$

²In section 3.4.3, surface temperature fluctuates and following time derivative, Eq. 3.14, is delicate.

$$f^{\text{wake}} = \pi r^2 P^{\text{wake}} \quad (3.20)$$

$$P^{\text{wake}} = \frac{-6}{\text{Re}} \left(\frac{\rho \ell u_{\text{pre}}^2}{2} \right) \frac{r_{\text{pre}}^2}{(y_{\text{pre}} - 2r)^2} - \frac{\rho \ell u_{\text{pre}}^2}{2} \frac{r_{\text{pre}}^3}{(y_{\text{pre}} - 2r)^3} \quad (3.21)$$

Using Oseen modifications [37], Eq. 3.21 determined wake pressure due to previous bubble (Zhang and Tan [38]).

Assumption 3.5 Temperature field on surface is expressed as superposition of normal distribution which peak is at each site.

$$T(l_1, l_2) = T_\infty + T_1 \exp\left(\frac{-l_1^2}{2\gamma^2}\right) + T_2 \exp\left(\frac{-l_2^2}{2\gamma^2}\right) \quad (3.22)$$

where T_∞ is temperature far from sites and l_1, l_2 are the distances from the nucleation sites 1 and 2. γ is the model constant determined from experimental data³. T_1 and T_2 are always negative due to coolings by vaporization.

Difference of enthalpy, ΔH , of superheated liquid layer and its time derivative is easily calculated as,

$$\Delta H = \int (\rho c_p \delta)_{\text{eff}} T(l_1, l_2) dS \quad (3.24)$$

$$= \int_0^\infty (\rho c_p \delta)_{\text{eff}} T_1 \exp\left(\frac{-l_1^2}{2\gamma^2}\right) 2\pi l_1 dl_1 \quad (3.25)$$

$$+ \int_0^\infty (\rho c_p \delta)_{\text{eff}} T_2 \exp\left(\frac{-l_2^2}{2\gamma^2}\right) 2\pi l_2 dl_2 \quad (3.26)$$

$$= 2\pi\gamma^2 (\rho c_p \delta)_{\text{eff}} (T_1 + T_2) \quad (3.27)$$

$$\dot{H} = 2\pi\gamma^2 (\rho c_p \delta)_{\text{eff}} (\dot{T}_1 + \dot{T}_2) \quad (3.28)$$

Assumption 3.6 Coalescence occurs when bubbles' edges touch.

Under this experimental conditions, bouncing rarely occurs. Therefore coalescence is simply geometrical problem and this assumption facilitate the modeling (Experimental study of the vapor bubble coalescence was conducted by Bonjour et al. [39] and Chen and Chung [40]). Coalescence often occurs if the cavities are closer as a matter of course.

³Dissipation equation tells us that conduction enlarge γ and time evolution of temperature field becomes a self-similar solution,

$$T = \frac{1}{4\pi t} \exp\left(\frac{-l^2}{4t}\right). \quad (3.23)$$

For simplicity, the effect of dissipation is approximately included as interaction through conductive heat transfer.

3.4.3 Phenomenological governing equation

In previous subsection, several assumptions and governing equations of a single site were described, then two sites are connected in this subsection.

Following equations, Eqs. 3.29 to 3.31 are governing equations corresponding to Eqs. 3.4 and 3.5.

$$\dot{r}_i = \frac{\pi\alpha}{8} \left(\frac{\rho_\ell c_{p,\ell}}{\rho_v h_{fg}} \right)^2 \frac{\Delta T_i^2}{r_i} \quad (i = 1, 2) \quad (3.29)$$

$$\dot{T}_i = \frac{1}{2\pi(\rho c \delta)_{\text{eff}} \gamma^2} (2\pi\gamma^2 q_{\text{in}} - \rho_v h_{fg} 4\pi r^2 \dot{r} + A_{\text{eff}} q_{\text{cond},i}) \quad (i = 1, 2) \quad (3.30)$$

$$\dot{y}_{\text{pre},i} = u_{\text{pre},i} \quad (i = 1, 2) \quad (3.31)$$

where

$$q_{\text{cond},1} = k_{\text{eff}} \frac{T_2 - T_1}{S} \quad (3.32)$$

$$q_{\text{cond},2} = -q_{\text{cond},1} = k_{\text{eff}} \frac{T_1 - T_2}{S} \quad (3.33)$$

q_{in} is input laser heat flux and subscripts “eff” means effective value which calculated from the properties of superheated liquid layer and silicon surface. q_{cond} is conductive heat transfer term of interaction term corresponding to $\mathbf{g}(\mathbf{x}_1, \mathbf{x}_2)$.

Conductive heat transfer is written as

$$q_{1 \rightarrow 2} = k_{\text{eff}} \frac{T_1 - T_2}{S} \quad (3.34)$$

k_{eff} is an effective thermal conductivity with liquid and solid. Nusselt number, Nu estimated from experimental data was

$$Nu = q_{\text{input}}/q_{1 \rightarrow 2} \simeq 0.1. \quad (3.35)$$

It means the conductive heat transfer is not negligible.

3.5 Model Behavior

Figure 3.8 is a model simulation results⁴ of bubbling period distribution and average bubbling frequency. It shows that period distribution of both

⁴It is a result of a model presented in an abstract which describes the time evolutions of a bubble radius, r_i , temperature, T_i and previous bubble height, y_i^{pre} of each site i .

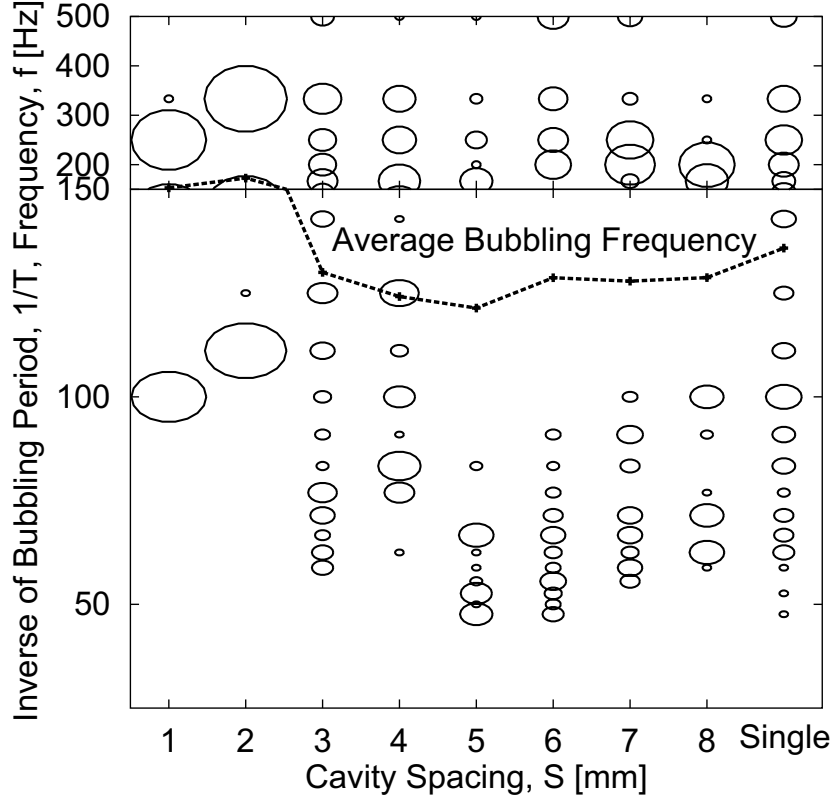


Figure 3.8: Bubbling period distribution (Model)

experiment (Fig. 3.3) and model simulation (Fig. 3.8) is divided into small

Model equations expressed in a proper dimensionless form are

$$\dot{r}_i = \frac{72 T_{\text{site},i}^2}{\pi^2 r_i} \quad (3.36)$$

$$\dot{T}_i = q - \dot{V}_{\text{bub},i}(r_i, \dot{r}_i) \quad (3.37)$$

$$\dot{y}_i^{\text{pre}} = u(r_i^{\text{pre}}) \quad (3.38)$$

$$\text{where } T_{\text{site},1} = T_1 + T_2 \exp\left(\frac{-S^2}{2\sigma^2}\right) \quad (3.39)$$

$$T_{\text{site},2} = T_2 + T_1 \exp\left(\frac{-S^2}{2\sigma^2}\right) \quad (3.40)$$

here dot means $\frac{d}{dFo}$ Eqs. 3.36 to 3.38 mean bubble growth rate derived from the study by Mikic et al. [34], energy conservation and previous bubble motion of each site, respectively. The superposed temperature of Eqs. 3.39 and 3.40, and bubble coalescence which is simply geometrical problem, connect the sites. Bubble departure is determined by balance of force acting on the bubble.

periods and large periods. Average bubbling frequency of the model was, however, calculated higher than that of experiment since vertical coalescence with preceding bubbles was more frequently occurred. Further improvement of the model will be required.

3.6 Concluding Remarks

Dynamical interaction between vapor bubble on nucleation sites was investigated experimentally and theoretically. In experiment, bubble departure periods were not constant value and distributed separately due to the vertical coalescence and wake effect of preceding bubble. It indicated that evaluation of interaction with average frequency is not efficient yet. a simple time dependent model was constructed to reveal the interaction and dominance of factors according to cavity spacing. The model consists of conduction, convection and coalescence simply as possible. Average bubbling frequency of the model was, however, calculated higher than that of experiment since vertical coalescence with preceding bubbles was more frequently occurred. Further discussion is needed.

Chapter 4

Conclusion

In isothermal twin orifices system, pressure difference derived from surface tension and inertial force drives the bubbling behavior. The three patterns take place according to the flow rate repeatedly.

In boiling system, period distribution as function of spacing was simulated by the model. More variables (degrees of freedom) than isothermal system were required for modeling even in such a simple system since thermal and hydrodynamical factors are strongly connected in boiling system. Bubble coalescence play the important role in actual boiling and this model, however mathematical discussion was postponed due to its discontinuity.

Future works are as follows. The models presented in this thesis describe a dynamical bubble behaviors as the forms of dynamical systems, $\dot{\mathbf{x}} = \mathbf{f}(\mathbf{x}; \mu)$. μ is a parameter, flow rate, q , in isothermal model or cavity spacing, S , in boiling model. Even though the model equations are determined, the alterations of parameter change the models' behaviors drastically due to the nonlinearities of the models. Given a specific dynamical systems, the studies of dynamical systems give a complete characterization of the geometry of the orbit structure. If the dynamical system depends on parameters, then they characterize the change in the orbit structure as the parameters are varied. Discussion from the standpoint of dynamical systems will be required.

Bibliography

- [1] M. Shoji. “light and shade in heat transfer research” — heart transferred to the research; in comfort, at ease, and with personality —. *Jour. HTSJ*, 37(146):106–108, 7 1998. (in Japanese).
- [2] V. P. Carey. *Liquid-Vapor Phase-Change Phenomena*. Hemisphere Publishing Corporation, 1992.
- [3] A. F. Mills. *Heat Transfer*. Prentice Hall, second edition, 1999.
- [4] Masahiro Shoji. Boiling chaos and modeling. In *11th International Heat Transfer Conference*, volume 1, pages 3–21, 1998.
- [5] Yuto Takagi and Masahiro Shoji. A simple bubbling model of a bubbling nucleation site. In *Proc. of 3rd organized multiphase flow forum '99 — Micro-scale structure of multiphase flows* —, pages 20–26, 1999. (in Japanese).
- [6] Masahiro Shoji. Studies of boiling chaos: a review. *Int. J. Heat Mass Transfer*, 47:1105–1128, 2004.
- [7] Shu Takagi, Norihiko Yamamoto, Takayoshi Inoue, and Kunio Hijikata. Behavior of a boiling bubble from a micro-scale heater. In *Proc. of 11th IHTC*, volume 2, pages 479–484, 1998.
- [8] Jost von Hardenberg, David B. R. Kenning, Huijuan Xing, and L. A. Smith. Nucleation site interactions. In *5th international conference on boiling heat transfer*, 2003.
- [9] Vijay K. Dhir. Numerical simulations of pool-boiling heat transfer. *AIChE J.*, 47:813–834, 2001.
- [10] Tatsuo Yanagita. Phenomenology of boiling: A coupled map lattice model. *Chaos*, 2(3):343–350, 1992.

-
- [11] Kunihiko Kaneko. Overview of coupled map lattices. *Chaos*, 2(3):279–282, 1992.
- [12] J. H. Ellepola and D. B. R. Kenning. Nucleation site interaction in pool boiling. In *Proc. 2nd european thermal-science and 14th UIT national heat transfer conference*, volume 3, pages 1669–1675, 1996.
- [13] Jerome Ellepola. *Nucleate boiling, nonlinaer spatio-temporal variations in wall temperature*. Ph. D Thesis, Oxford University, 1997.
- [14] Masahiro Shoji and Yuto Takagi. Bubbling features from a single artificial cavity. *Int. J. Heat Mass Transfer*, 44:2263–2276, 2001.
- [15] Masahiro Shoji and Lei Zhang. Boiling features on artificial surfaces. In *5th international conference on boiling heat transfer*, 2003.
- [16] Surapong Chatpun, Makoto Watanabe, and Masahiro Shoji. Nucleation site interaction in pool nucleate boiling on a heated surface with triple artificial cavities. *Int. J. Heat Mass Transfer*, 2004. (in press).
- [17] Edward N. Lorenz. Deterministic nonperiodic flow. *J. atmos. Sci*, 20:130–141, 1963.
- [18] R. Clift, J. R. Grace, and M. E. Weber. *Bubbles, Drops and Particles*. Academic Press, 1978.
- [19] Louis John Mittoni, Mark Philip Schwarz, and Robert David La Nauze. Deterministic chaos in the gas inlet pressure of gas-liquid bubbling system. *Phys. Fluids*, 7(4):891–893, 1995.
- [20] D. J. Tritton and C. Egdell. Chaotic bubbling. *Phys. Fluids A*, 5:503–505, 2 1993.
- [21] Masahiro Shoji. Nonlinear bubbling and micro-convection at a submerged orifice. *Tsinghua Science and Technology*, 7(2):97–108, 4 2002.
- [22] Lei Zhang and Masahiro Shoji. Aperiodic bubble formation from a submerged orifice. *Chem. Eng. Sci.*, 56:5371–5381, 2001.
- [23] G. Titomanlio, G. Rizzo, and D. Acierno. Gas bubble formation from submerged orifices — “simultaneous bubbling” from two orifices. *Chem. Eng. Sci.*, 31:403–404, 1976.
- [24] M. Ruzicka, J. Drahoš, J. Zahradník, and N. H. Thomas. Structure of gas pressure signal at two-orifice bubbling from a common plenum. *Chem. Eng. Sci.*, 55:421–429, 2000.

-
- [25] Andrzej Calka and Ross L. Judd. Some aspects of the interaction among nucleation sites during saturated nucleate boiling. *Int. J. Heat Mass Transfer*, 28(12):2331–2342, 1985.
- [26] Lei Zhang and Masahiro Shoji. Nucleation site interaction in pool boiling on the artificial surface. *Int. J. Heat Mass Transfer*, 46:513–522, 2003.
- [27] Milton S. Plesset and Andrea Prosperetti. Bubble dynamics and cavitation. In *Ann. Rev. Fluid. Mech.*, volume 9, pages 145–185. Annual Reviews Inc., 1977.
- [28] Pierre-Gilles de Gennes, Françoise Brochard-Wyart, and David Quéré. *Capillarity and Wetting Phenomena: drops, bubbles, pearls, waves*. Springer-verlag, 2003.
- [29] Iztok Golobič and Henrik Gjerkeš. Interactions between laser-activated nucleation sites in pool boiling. *Int. J. Heat Mass Transfer*, 44:143–153, 2001.
- [30] T. G. Theofanous, J. P. Tu, A. T. Dinh, and T. N. Dinh. The boiling crisis phenomenon part i: nucleation and nucleate boiling heat transfer. *Experimental Thermal and Fluid Science*, 26:775–792, 2002.
- [31] D. B. R. Kenning and Youyou Yan. Investigation of boiling heat transfer by liquid crystal thermography. *Experimental Thermal and Fluid Science*, 25:219–229, 2001.
- [32] R. Mosdorf and M. Shoji. Chaos in nucleate boiling — nonlinear analysis and modeling. *Int. J. Heat Mass Transfer*, 47:1515–1524, 2004.
- [33] Yoshiro Katto and Sadao Yokoya. Behavior of a vapor mass in saturated nucleate and transition pool boiling. *Heat Transfer Japanese Research*, 5(2):45–65, 1976.
- [34] B. B. Mikic, W. M. Rohsenow, and P. Griffith. On bubble growth rates. *Int. J. Heat Mass Transfer*, 13:657–666, 1970.
- [35] Robert Cole and Herman L. Shulman. Bubble growth rates at high jakob numbers. *Int. J. Heat Mass Transfer*, 9:1377–1390, 1966.
- [36] D. J. McCann and R. G. H. Prince. Bubble formation and weeping at a submerged orifice. *Chem. Eng. Sci.*, 24:801–814, 1969.
- [37] H. Lamb. *Hydrodynamics*. Cambridge university press, 6th edition, 1945.

- [38] Wenxing Zhang and R. B. H. Tan. A model for bubble formation and weeping at a submerged orifice. *Chem. Eng. Sci.*, 55:6243–6250, 2000.
- [39] Jocelyn Bonjour, Marc Clausse, and Monique Lallemand. Experimental study of the coalescence phenomenon during nucleate pool boiling. *Experimental Thermal and Fluid Science*, 20:180–187, 2000.
- [40] Tailian Chen and J. N. Chung. Coalescence of bubbles in nucleate boiling on microheaters. *Int. J. Heat Mass Transfer*, 46:513–522, 2003.

以上

1 - 50 ページ 完

修士論文

平成 16 年 2 月 13 日 提出

26177 丹下 学